Coupling of Surface Plasmons and Excited Optical Modes in Metal/Dielectric Grating Stacks

Ren-Hao Fan, Dong-Xiang Qi, Qing Hu, Ling Qin, Ru-Wen Peng*, and Mu Wang

National Laboratory of Solid State Microstructures and Department of Physics,
Nanjing University, Nanjing 210093, China

In this work, we investigate the coupling of surface plasmons and excited optical modes in metal/dielectric grating stacks theoretically and experimentally. We have observed three kinds of modes in these structures: the cavity mode, the propagated surface plasmon (PSP) mode and the localized surface plasmon (LSP) mode, which can enhance the optical transmission. Firstly, it is shown that the cavity mode is excited in the grating stacks. And the cavity mode has redshift if we enhance the thickness of metal layers, while it has blueshift when we increase the thickness of dielectric layers. The redshift of the cavity mode also occurs when the number of repeating layers is increased. Secondly, the PSP mode is also excited, which can be described by the effective permittivity method. It is found that the PSP modes are coupled with each other, which leads to a modified dispersion relation of surface plasmon polaritons (SPP). The theoretical analysis is in good agreement with the observed transmission enhancement in the grating stacks. And the coupling of PSPs also leads to a blueshift when the number of metal layers is increased. Thirdly, the LSP mode, generated in single metal strip, can also enhance the optical transmission of the grating stacks. Yet the transmission intensity induced by LSP decreases rapidly with increasing the number of metal layers. The investigations here may have potential applications in designing plasmonic metamaterials and subwavelength optical devices.

Keywords: Surface Plasmons, Optical Transmission, Subwavelength Grating.

1. INTRODUCTION

In the past decade, much attention has been paid to plasmonics and subwavelength optics.[1,2] Subwavelength grating is one of the simple and interesting systems, and several theoretical and experimental works are performed to study its optical transmission.[3–5] Two types of transmission resonances which can cause perfect transmission were reported in Porto et al.'s theoretical work: coupled SPP's on both horizontal surfaces of the metallic grating, and cavity modes located inside the slits.[4] Very recently, nearly perfect Fano transmission resonances through nanoslits drilled in a metallic membrane have been observed experimentally.[6] The coupling strength between SPP and transmitted light in metallic nanoslit structures is found to be the product of the geometric opening ratio, the aperture momentum, and the Fabry-Perot factor.[7] A charge oscillation-induced light emission mechanism is also reported to explain the extraordinary optical transmission from the electronic scale,[8] and we find that metallic gratings consisting of narrow slits may become transparent for extremely broad

bandwidths under oblique incidence.[9] Rich physics and potential applications (such as flat-panel display,[10] generator of terahertz electromagnetic radiation[11] and plasmonic laser.[12]) are attracting more researches on transmission gratings.

Some groups have reported that in the gratings with double metal layers, they can control the coupling of modes between two metal layers by changing the thickness of dielectric layer.[13,14] However, adjusting the number of the metal layers in transmission gratings has not been paid much attention yet. Physically, change the number of the metal layers may have an influence on the coupling of surface plamons,[15] which definitely affect the optical properties of the grating stacks. In this work, we investigate the coupling of surface plasmons and excited optical modes in metal/dielectric grating stacks theoretically and experimentally. In experiments, we have observed three kinds of modes in these structures: the cavity mode, the PSP mode and the LSP mode, which enhance the optical transmission. Based on the finite-difference time-domain (FDTD) method and the equivalent LC circuit model, we have carried out the theoretical calculations, which are in good agreement with the experimental results.

---

*Author to whom correspondence should be addressed.
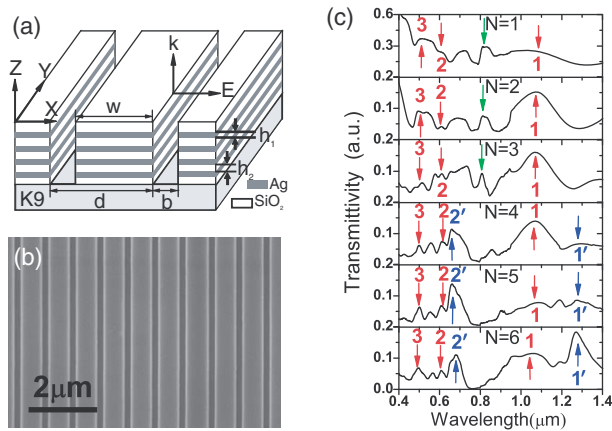
Fig. 1. (a) The schematic diagram of the grating with four silver films ($N = 4$) and five silicon dioxide films. (b) SEM images of this grating ($N = 4$). (c) The experimentally transmission spectra of normal incident TM wave for gratings with parameters N from 1 to 6. There are three kinds of modes in these structures: the cavity mode marked by blue arrow, the PSP mode marked by red arrow, and the LSP mode marked by green arrow. In each structure, $d = 800$ nm, $b = 200$ nm, $h_1 = 35$ nm, $h_2 = 50$ nm.

2. EXPERIMENTAL DETAILS

We study several samples of Ag/SiO$_2$ grating stacks, which have different number of metal layers. In the following investigation, we use the parameter $N = 1, 2, 3, 4, 5, 6$ to distinguish different structures, which have the repeating number of silver films as 1, 2, 3, 4, 5, 6, together with one more silicon dioxide films. The schematic diagram of sample with four silver films and five silicon dioxide films expressed by $N = 4$ is shown in Figure 1(a) as an example. Our samples have the same period of $d = 800$ nm, the same slit width of $b = 200$ nm, and the same strip width expressed by w. Each silver film has the thickness of $h_1 = 35$ nm and the thickness of silicon dioxide film is $h_2 = 50$ nm.

The Ag/SiO$_2$ grating stacks have been fabricated in the following way. Firstly, silicon dioxide film with the thickness of 50 nm was coated on the substrate of K9 optical glass by magnetron sputtering technique. Then, 35 nm silver and 50 nm silicon dioxide films construct, and the repeating number of building blocks is $N = 1, 2, 3, 4, 5, 6$ in the different stacks, respectively. Finally, focused-ion-beam facility (strata FIB 201, FEI company, 30 keV Ga ions) was used to mill the grating structure. As an example, Figure 1(b) shows the SEM image of the Ag/SiO$_2$ grating stack with $N = 4$, which was measured by field-emission scanning-electron microscope. Microspectrophotometer (Craic, QDI2010) was used to measure the optical spectra of the samples.

3. RESULTS AND DISCUSSION

The experimentally transmission spectra of normal incident TM wave (***E//x***) for the structures with parameters

N from 1 to 6 are shown in Figure 1(c). First of all, we find that the two cavity modes, which are marked by the blue arrow, only appear when $N > 3$. The reason is that the cavity modes exist only when the height of the groove is significantly larger than the width of the groove. The resonance wavelengths of these cavity modes have redshift when N is increased. Secondly, the PSP modes, which are marked by the red arrow, are found in transmission spectra. When the layers are increased from $N = 1$ to $N = 6$, the PSP modes have blueshift because of the coupling of SPs.[15] The intensity of PSP modes declined when increasing the layers. In the third, the LSP modes, which are marked by the green arrow, are observed in these periodic structures. Their resonance wavelengths do not change when increasing the layers. But their transmission intensity declined rapidly so that the LSP cannot be observed when $N > 3$.

Next we theoretically investigate the above three kinds of optical modes based on the finite-difference time-domain (FDTD) method as following. The calculated transmission spectra of normal incident TM wave (***E//x***) for structures with parameters N from 1 to 6 are shown in Figure 2(a). In each structure, $d = 800$ nm, $b = 200$ nm, $h_1 = 35$ nm, $h_2 = 50$ nm. Cavity modes appear when the height of the groove is significantly larger than the width of the groove. They only appear in these structures when $N > 3$. Here exist two cavity modes in the visible and near-infrared ranges of these structures as marked by the blue arrow in Figure 2(a). The fundamental cavity mode is labeled with number "1′", and the mode with approximate twice the frequency of the fundamental mode is labeled in number "2′". Figure 2(b) illustrates the electric field distributions of the fundamental cavity mode in the grating with $N = 4$ at the wavelength of 1233 nm. Base on these
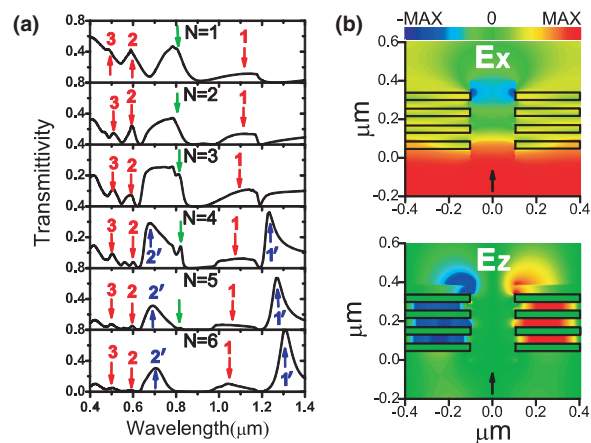
Fig. 2. (a) The calculated transmission spectra of normal incident TM wave for structures with parameters N from 1 to 6. In each structure, $d = 800$ nm, $b = 200$ nm, $h_1 = 35$ nm, $h_2 = 50$ nm. (b) The electric field (E_x along the X axis, E_z along the Z axis) of the fundamental mode in grating with four silver layers ($N = 4$) at wavelength of 1233 nm. The black arrow indicates the direction of the incidence, and the boundaries of silver films are marked by black line.

field distributions, we can use the equivalent LC circuit model to discuss the resonance condition for the fundamental cavity mode.

The equivalent LC circuit of the structure containing four metal layers ($N = 4$) can be given as Figure 3(a). Equivalent inductance comes from two parts. The first part L_m represents the equivalent inductance of two parallel strips and it can be expressed as $L_m = 0.5\mu_0 h_1 b/l$,[16, 17] where μ_0 is the vacuum permeability and l is the strip length in the y direction. The second part comes from the contribution of the drifting electrons which is given by $L_e = h_1/(\varepsilon_0 \omega_p^2 \delta l)$,[17] where $\omega_p = 1.364 \times 10^{16}$ rad/s is the plasma frequency of Ag.[18] The effective cross-sectional area of the metal strip is approximated as δl by assuming that all induced electric current flows at the depths within the power penetration depth δ. Here the power penetration depth is set to be 13 nm for simplicity because the fundamental mode locates at the near-infrared range. Equivalent capacitance also comes from two parts. The electric field along the X axis is mainly concentrated at the edge of the cavity between silver strips. So equivalent capacitance comes from the edge of the cavity can be described as $C_0 = f\varepsilon_{air}\varepsilon_0 h_1 l/b$, where f is the correction factor of parallel-plate capacitor. The electric field along the Z axis is mainly concentrated between silver layers, so equivalent capacitance between silver layers can be described as $C_m = 0.5\varepsilon_{sio_2}\varepsilon_0 wl/h_2$. The total impedance of this LC circuit with N layers of silver films can be expressed as $Z_{Ntot} = i[2N\omega_N(L_m + L_e) - 2(\omega_N C_0)^{-1} - 2(N-1)(\omega_N C_m)^{-1}]$, where N is an integer. This formula

establish in these gratings of this article when $N > 3$. When $Z_{Ntot} = 0$, we can get the fundamental mode which can be expressed as follows:

$$\omega_N^2 = \frac{1/C_0 + (N-1)/C_m}{N(L_m + L_e)} \quad (1)$$

From Eq. (1), we can find that there is no correlation between the frequency of the fundamental cavity mode and the strip length l. So we set $l = 1$ m in the following discussion for simplicity. Equation (1) can be expressed as: $N\omega_N^2 (L_m + L_e) = 1/C_0 + (N-1)/C_m$. The $1/C_m$ can be calculated from the structural parameters as $1/C_m = 8.714$ nF^{-1}. So if the assumptions are reasonable, $N\omega_N^2 (L_m + L_e)$ and $N - 1$ would have a linear relation with slope of $1/C_m = 8.714$ nF^{-1}. The fitting data show that: $N\omega_N^2 (L_m + L_e)$ and $N - 1$ have a good linear relation with slope of $1/C_m = (8.540 \pm 0.178)$ nF^{-1}, which agrees well with the calculating results from structural parameters, where fitting constant is $1/C_0 = (31.171 \pm 1.023)$ nF^{-1}.

The cavity modes have redshift when increasing the number of layers shown in Figure 2(a), because the length of the resonance cavity is increased. However, increasing the length of the resonance cavity cannot always cause cavity modes redshift. We find an interesting deduction from Eq. (1), that is, the cavity mode has blueshift when increasing the thickness of silicon dioxide film without changing other conditions. Figure 3(b) shows that the cavity mode has blueshift when the thickness of silicon dioxide film is increased, and this result mainly comes from that the equivalent capacitance between metal layers is reduced. Meanwhile, increasing the thickness of silver film, but not changing other conditions, can increase the equivalent inductance. As a result, the cavity mode will have redshift according to Eq. (1), which is demonstrated in Figure 3(c). Therefore, we can tune the cavity mode by changing the thickness of silicon dioxide film and silver film.

It is well known that at the interface separating a metal and a dielectric, the PSP mode obeys the following dispersion relation: $k_{sp} = k_0[\varepsilon_d\varepsilon_m/(\varepsilon_d + \varepsilon_m)]^{1/2}$, where k_0 is the wave vector of the incident light, ε_d is the permittivity of the dielectric, and ε_m is the permittivity of the metal. We find that the dispersion relation of SPP for a flat interface should be modified when it is used for 1D metal grating system. Because of the presence of the air groove, the interface is no longer separating a metal and a dielectric but mixing with air layer, which changes the effective permittivity of both dielectric and metal. Here we use the effective permittivity method to modify the dispersion of SPP. The effective dielectric permittivity ε_{deff} can be given by: $\varepsilon_{deff} = P\varepsilon_{sio_2} + (1 - P) \varepsilon_{air}$,[19, 20] where ε_{sio_2} and ε_{air} are the dielectric permittivities of silicon dioxide and air respectively, and $P = w/d$ is defined as the duty cycle of grating. As to the effective metal permittivity ε_{meff} of the grating structure described in this paper, we give the following empirical formula: $\varepsilon_{meff} = P\varepsilon_m + (1 - P)\varepsilon_{air}$, where
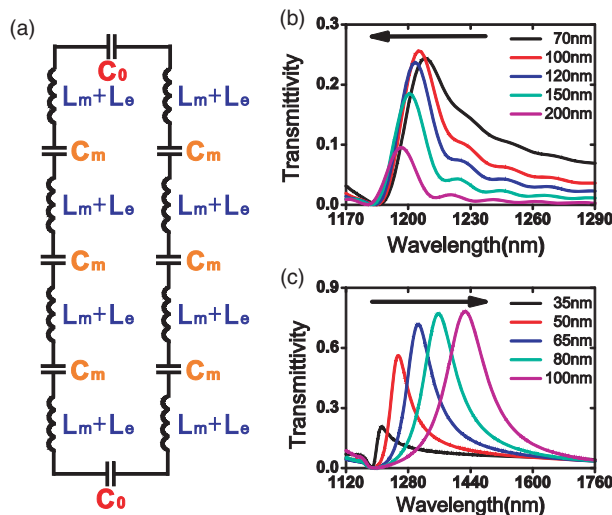
Fig. 3. (a) The equivalent LC circuit of the structure containing four metal layers ($N = 4$). (b) The zero-order transmission spectra of the fundamental mode of structures $N = 4$, with different thickness of silicon dioxide film as 70 nm, 100 nm, 120 nm, 150 nm, and 200 nm, respectively. These gratings have the same $d = 800$ nm, $b = 200$ nm and $h_1 = 35$ nm. (c) The zero-order transmission spectra of the fundamental mode of structures $N = 4$, with different thickness of silver films as 35 nm, 50 nm, 65 nm, 80 nm, and 100 nm, respectively. All the gratings have the same $d = 800$ nm, $b = 200$ nm and $h_2 = 50$ nm.

ε_m is the permittivity of the metal. This modification does not violate the condition for the existence of SPP modes, in which the real part of the effective metal permittivity is negative.[21] The reason is that the negative real part of ε_m is much greater than the positive real part of ε_{air} in the visible and nearinfrared ranges. The frequency-dependent permittivity of silver is based on the Lorentz-Drude model,[22] and the permittivity of silicon dioxide is taken as $\varepsilon_{sio_2} = 2.16$. We obtain the wavelength of SPP modes satisfying:

$$\lambda = \frac{d}{m} \sqrt{\frac{\varepsilon_{deff} \varepsilon_{meff}}{\varepsilon_{deff} + \varepsilon_{meff}}} \qquad (2)$$

Based on Eq. (2), three PSP modes marked by the red arrow in Figure 2(a) can be indexed by $m = 1, 2, 3$, respectively. The PSP modes have blueshift and their intensity declined when layers are increased because of the coupling of SPs. Electric fields are enhanced at the surface of every metal strip and interact with each other, which leads to blueshift of the PSP mode.

Figure 4(a) shows the transmission spectra of structures with 35 nm thickness silver film and surrounded with two 50 nm thickness silicon dioxide films. The widths of these strips are 400 nm, 500 nm, 600 nm, 700 nm, and 800 nm, respectively. The transmission peaks are marked by green arrow. The electric field distribution of the mode of the strip with width of 600 nm at wavelength of 810 nm is shown in Figure 4(b). The local electric field is enhanced on the surface of the silver strip and radiates to its surrounding medium in a very short range, which is similar to the LSP mode.[23] We find that the resonance wavelengths of these LSP modes are increased as the strips widen, because the LSP mode strongly depends on the geometry of the object.[23, 24] For the periodic structure, we find

that the electric field distribution of the mode marked by green arrow in Figure 2(a) is similar to the mode in the 600 nm width strip structure in Figure 4(a). The LSP mode maintains the same resonance wavelength in the 1D grating structure compare with single metal strip, because they have the same geometry. Therefore, LSP mode of single metal strip can also exist in grating structures. Their transmission intensities decline rapidly when the number of metal layers is increased, because of strong attenuation of radiation from one metal layer to the other.

4. CONCLUSIONS

In this work, we find three kinds of modes in metal/dielectric grating stacks as the cavity mode, the PSP mode and the LSP mode, which enhance the optical transmission. Firstly, the cavity mode has redshift if we increase the thickness of metal layers; while it has blueshift when we increase the thickness of dielectric layers. The redshift of the cavity mode also occurs when the number of repeating layers is increased. Secondly, the PSP mode of the grating structure can be described by the effective permittivity method. And the coupling of PSPs also leads to a blueshift when the number of metal layers is increased. In the third, the LSP mode which generated in single metal strip can also enhance the optical transmission of the grating stacks. Yet the transmission intensity induced by LSP decreases rapidly with increasing the number of metal layers. The investigations here may have potential applications in designing plasmonic metamaterials and subwavelength optical devices.

References and Notes

1. T. W. Ebbesen, H. J. Lezec, H. F. Ghaemi, T. Thio, and P. A. Wolff, *Nature* 391, 667 (**1998**).
2. F. Gao, J. Z. Zhao, D. X. Qi, Q. Hu, R. L. Zhang, and R. W. Peng, *J. Nanosci. Nanotechnol.* 10, 7324 (**2010**).
3. U. Schröter and D. Heitmann, *Phys. Rev. B* 58, 15419 (**1998**).
4. J. A. Porto, F. J. García-Vidal, and J. B. Pendry, *Phys. Rev. Lett.* 83, 2845 (**1999**).
5. F. J. García-Vidal and L. Martín-Moreno, *Phys. Rev. B* 66, 155412 (**2002**).
6. S. Collin, G. Vincent, R. Haïdar, N. Bardou, S. Rommeluère, and J. L. Pelouard, *Phys. Rev. Lett.* 104, 027401 (**2010**).
7. K. G. Lee and Q. H. Park, *Phys. Rev. Lett.* 95, 103902 (**2005**).
8. X. R. Huang, R. W. Peng, Z. Wang, F. Gao, and S. S. Jiang, *Phys. Rev. A* 76, 035802 (**2007**).
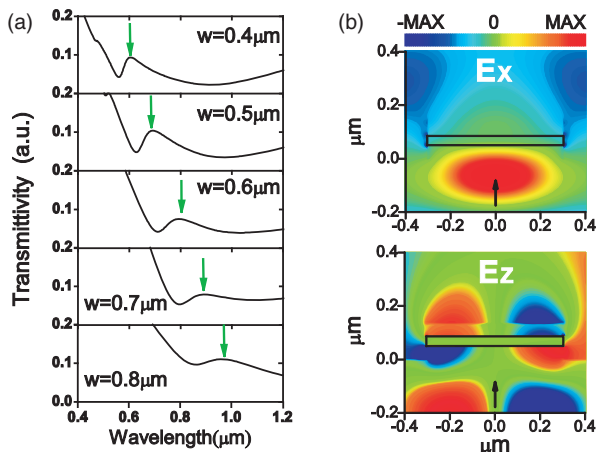
Fig. 4. (a) The transmission spectra of normal incidence for structures with 35 nm thickness silver film and surrounded with two 50 nm thickness silicon dioxide films. The widths of these strips are 400 nm, 500 nm, 600 nm, 700 nm and 800 nm, respectively. The LSP mode is marked by the green arrow. (b) The electric field (E_x along the X axis, E_z along the Z axis) of the LSP mode of the strip with width of 600 nm at wavelength of 810 nm.

9. X. R. Huang, R. W. Peng, and R. H. Fan, *Phys. Rev. Lett.* 105, 243901 (**2010**).
10. N. Fang, H. Lee, C. Sun, and X. Zhang, *Science* 308, 534 (**2005**).
11. G. H. Welsh, N. T. Hunt, and K. Wynne, *Phys. Rev. Lett.* 98, 026803 (**2007**).
12. X. F. Li, S. F. Yu, and A. Kumar, *Appl. Phys. Lett.* 95, 141114 (**2009**).
13. C. Cheng, J. Chen, D. J. Shi, Q. Y. Wu, F. F. Ren, J. Xu, Y. X. Fan, J. P. Ding, and H. T. Wang, *Phys. Rev. B* 78, 075406 (**2008**).
14. Y. H. Ye, Y. W. Jiang, M. W. Tsai, Y. T. Chang, C. Y. Chen, D. C. Tzuang, Y. T. Wu, and S. C. Lee, *Appl. Phys. Lett.* 93, 263106 (**2008**).
15. Z. H. Tang, R. W. Peng, Z. Wang, X. Wu, Y. J. Bao, Q. J. Wang, Z. J. Zhang, W. H. Sun, and Mu Wang, *Phys. Rev. B* 76, 195405 (**2007**).
16. J. F. Zhou, E. N. Economon, T. Koschny, and C. M. Soukoulis, *Opt. Lett.* 31, 3620 (**2006**).
17. L. P. Wang and Z. M. Zhang, *Appl. Phys. Lett.* 95, 111904 (**2009**).
18. J. Zhou, T. Koschny, M. Kafesaki, E. N. Economou, J. B. Pendry, and C. M.Soukoulis, *Phys. Rev. Lett.* 95, 223902 (**2005**).
19. L. Poladian, *Phys. Rev. B* 44, 2092 (**1991**).
20. R. Brauer and O. Bryngdahl, *Appl. Opt.* 33, 7875 (**1994**).
21. A. V. Zayats, I. I. Smolyaninov, and A. A. Maradudin, *Phys. Rep.* 408, 131 (**2005**).
22. A. D. Rakic, A. B. Djurisic, J. M. Elazar, and M. L. Majewski, *Appl. Opt.* 37, 5271 (**1998**).
23. J. P. Kottmann, O. J. F. Martin, D. R. Smith, and S. Schultz, *Phys. Rev. B* 64, 235402 (**2001**).
24. J. S. Yu, M. Kim, S. Kim, D. H. Ha, B. H. Chung, S. J. Chung, and J. S. Yu, *J. Nanosci. Nanotechnol.* 8, 4548 (**2008**).

RESEARCH ARTICLE